Original Article | Musculoskeletal Imaging

eISSN 2005-8330
https://doi.org/10.3348/kjr.2021.0140
Korean J Radiol 2021;22(11):1850-1857

Korean Journal of Radiology
KJR

Deep Learning Algorithm for Simultaneous Noise Reduction and Edge Sharpening in Low-Dose CT Images: A Pilot Study Using Lumbar Spine CT

Hyunjung Yeoh[1], Sung Hwan Hong[1], Chulkyun Ahn[2], Ja-Young Choi[1], Hee-Dong Chae[1], Hye Jin Yoo[1], Jong Hyo Kim[1, 2, 3]

[1]Department of Radiology, Seoul National University College of Medicine, Seoul, Korea; [2]Department of Transdisciplinary Studies, Program in Biomedical Radiation Sciences, Graduate School of Convergence Science and Technology, Seoul National University, Seoul, Korea; [3]Center for Medical-IT Convergence Technology Research, Advanced Institutes of Convergence Technology, Suwon, Korea

Objective: The purpose of this study was to assess whether a deep learning (DL) algorithm could enable simultaneous noise reduction and edge sharpening in low-dose lumbar spine CT.

Materials and Methods: This retrospective study included 52 patients (26 male and 26 female; median age, 60.5 years) who had undergone CT-guided lumbar bone biopsy between October 2015 and April 2020. Initial 100-mAs survey images and 50-mAs intraprocedural images were reconstructed by filtered back projection. Denoising was performed using a vendor-agnostic DL model (ClariCT.AI™, ClariPI) for the 50-mAS images, and the 50-mAs, denoised 50-mAs, and 100-mAs CT images were compared. Noise, signal-to-noise ratio (SNR), and edge rise distance (ERD) for image sharpness were measured. The data were summarized as the mean ± standard deviation for these parameters. Two musculoskeletal radiologists assessed the visibility of the normal anatomical structures.

Results: Noise was lower in the denoised 50-mAs images (36.38 ± 7.03 Hounsfield unit [HU]) than the 50-mAs (93.33 ± 25.36 HU) and 100-mAs (63.33 ± 16.09 HU) images ($p < 0.001$). The SNRs for the images in descending order were as follows: denoised 50-mAs (1.46 ± 0.54), 100-mAs (0.99 ± 0.34), and 50-mAs (0.58 ± 0.18) images ($p < 0.001$). The denoised 50-mAs images had better edge sharpness than the 100-mAs images at the vertebral body (ERD; 0.94 ± 0.2 mm vs. 1.05 ± 0.24 mm, $p = 0.036$) and the psoas (ERD; 0.42 ± 0.09 mm vs. 0.50 ± 0.12 mm, $p = 0.002$). The denoised 50-mAs images significantly improved the visualization of the normal anatomical structures ($p < 0.001$).

Conclusion: DL-based reconstruction may enable simultaneous noise reduction and improvement in image quality with the preservation of edge sharpness on low-dose lumbar spine CT. Investigations on further radiation dose reduction and the clinical applicability of this technique are warranted.

Keywords: *DL; Noise reduction; Lumbar spine; Computed tomography*

INTRODUCTION

With more anatomical and diagnostic information, low-dose CT (LDCT) of the lumbar spine provides better image quality than lumbar spine radiography at a similar radiation level [1]. LDCT of the lumbar spine has been investigated

Received: February 17, 2021 **Revised:** May 27, 2021 **Accepted:** June 1, 2021
This work was supported by the Korea Medical Device Development Fund grant funded by the Korea government (the Ministry of Science and ICT, the Ministry of Trade, Industry and Energy, the Ministry of Health & Welfare, the Ministry of Food and Drug Safety) (Project Number: KMDF_PR_20200901_0017, 9991007051). This research was also supported by a grant of the Korea Health Technology R&D Project through the Korea Health Industry Development Institute (KHIDI), funded by the Ministry of Health & Welfare, Republic of Korea (grant number: HI20C2092).

Corresponding author: Sung Hwan Hong, MD, PhD, Department of Radiology, Seoul National University College of Medicine, 101 Daehak-ro, Jongno-gu, Seoul 03080, Korea.
• E-mail: drhong@snu.ac.kr

Korean Journal of Radiology
KJR

for evaluating traumatic and non-traumatic spinal diseases, and iterative reconstruction (IR) has been integrated into the LDCT protocol to further improve image quality [2-5].

To date, various CT technologies have been developed to reduce radiation doses and maintain image quality [6]. IR techniques implemented in LDCT reduce image noise and increase the signal-to-noise ratio (SNR); however, these techniques result in a reduction in subjective image sharpness [7]. Although this reduction in image sharpness may be tolerable in the imaging of the brain or abdomen, it can be a problem when interpreting a musculoskeletal CT where the bones and surrounding soft tissues create a high-contrast interface [8]. Therefore, when designing the LDCT protocol for the lumbar spine, it is necessary to not only reduce noise but also maintain image sharpness.

Another limitation of the IR techniques is that they are vendor-specific according to their application choices and compatible with only the latest scanners. In practice, a vendor-neutral option may be preferable because there are various types of CT models produced by multiple CT manufacturers [9]. A recently proposed deep learning (DL)-based denoising technique adopted for coronary CT angiography and chest CT showed both the vendor-neutral capability and clinical applicability with image sharpness preservation [10,11].

In our institution, when performing a CT-guided lumbar spine biopsy, the initial survey CT scan was obtained at 100 mAs, and the CT scan to guide biopsy needle placement was obtained at 50 mAs. Hence, we had a real dataset of lumbar CT images obtained at two different radiation doses from the same patient. Using this dataset, this study aimed to investigate whether the DL algorithm could enable simultaneous noise reduction and image sharpness preservation on LDCT of the lumbar spine.

MATERIALS AND METHODS

Study Population

This retrospective study was approved by our Institutional Review Board, which waived the requirement for informed consent from all the patients (IRB No. H-2006-177-1135). Between October 2015 and April 2020, 95 CT-guided lumbar spine biopsies were performed. Because the field of view (FOV) affects the quality of the CT image, 38 cases in which the FOV difference between the initial survey CT images and the intraprocedural CT images exceeded 10% were excluded. Four cases in which the levels of the initial survey CT images and intraprocedural CT images did not match were excluded. One case was excluded because the artifacts caused by motion were too severe. A total of 52 patients (26 male and 26 female; median age, 60.5 years; range, 37–87 years) were included.

Image Acquisition

All the patients were scanned using a 64-MDCT scanner (Brilliance 64, Philips Healthcare) at a tube voltage of 120 kVp. All the images were reconstructed in 2.5-mm axial slices using a filtered back-projection algorithm with a bone kernel. During the procedure, the initial survey CT images were obtained at 100 mAs, and the intraprocedural CT images were obtained at 50 mAs. Datasets of 10–16 consecutive axial images obtained at 100 mAs and 50 mAs were used for the analysis. The other CT parameters were as follows: gantry rotation time, 500 ms; detector collimation, 0.625 mm; detector pitch, 1.015; FOV, 139–377 mm for the initial survey CT and 140–372 mm for the intraprocedural CT; and matrix size, 512 x 512.

Denoise Processing

A DL-based reconstruction from the filtered back-projection images obtained at 50 mAs was performed using a commercially available DL model (DLM; ClariCT.AI, ClariPI), and the performance of DLM has been assessed in previous studies [10-16]. The DLM is an image-based CT denoising solution that uses a U-net-based convolutional neural net (CNN) architecture composed of contracting and expansive paths. The ensemble technique can increase accuracy, but it was not applied because it is disadvantageous in that the amount of calculation is increased. The DLM was trained with diverse vendor-specific LDCT images from different vendors to acquire generalized learning and vendor-agnostic denoising capability. The training dataset consisted of more than 1 million CT images encompassing 2100 different combinations of scan and reconstruction conditions, including varying kV, mAs, automatic exposure control, slice thickness, contrast enhancement, and convolution kernels with 24 scanner models from four major CT manufacturers (GE Healthcare, Siemens, Philips Healthcare, and Cannon). Among them, 80% of the datasets were used for model training, whereas the remaining 20% were used for validation. In addition, external validation was performed in four independent clinical studies. To prepare the training dataset, a synthetic sinogram-based LDCT simulation technique was used to generate a paired set of LDCT images

 https://doi.org/10.3348/kjr.2021.0140

and standard-dose CT images from a set of standard-dose CT images. The denoising speed was approximately 5 images/s on a computer equipped with a 3.0-GHz i7-9700 CPU and an NVIDIA GeForce RTX 2080 GPU.

Quantitative Image Analysis

As objective indexes for the image quality analysis, 1) image noise, 2) SNR, and 3) edge rise distance (ERD) were measured or assessed for each CT image. A circular region of interest (ROI) of a radius of 50–55 mm^2 was drawn on the paraspinal muscle by a board-certified musculoskeletal radiologist. Within the intraprocedural scan range, the level with the largest cross-sectional area of the paraspinal muscle without artifacts due to the biopsy needle was selected to draw the ROI. The ROIs were placed at the same location in the 50-mAs, denoised 50-mAs, and 100-mAs CT images. To minimize bias from a single measurement, the average value was obtained after drawing the ROI three times. Image noise was defined as the standard deviation of the Hounsfield units (HUs) within the region. The SNR was calculated by dividing the mean attenuation of the paraspinal muscle by the previously obtained image noise. The ERD was calculated for the objective evaluation of the image sharpness. The ERD represents the distance between two points at 10% and 90% of the maximal HU across a structural border (Fig. 1). A shorter ERD indicates a higher sharpness of the image. To measure the ERD, multiple short-line segments were drawn perpendicular to the margin of the vertebral body and the psoas muscle on each CT image. The edge line profiles along the short-line segments were automatically extracted, averaged, and plotted using MATLAB software programmed with MATrix LABoratory (MathWorks) [10,11].

Qualitative Image Analysis

Qualitative image analysis was performed with a bone window setting (window width of 4000 HU and window level of 500 HU) and a soft tissue window setting (window width, 400 HU; window level, 30 HU) using a PACS viewer. In a single session, two musculoskeletal radiologists with 6 and 27 years of experience in lumbar spine CT who were blinded to the tube current independently graded the overall image quality, which was modified from a previously published noise scoring system [17]. The visibility of anatomical structures was also evaluated using a 4-point ranking scale (Table 1). The seven anatomical regions for analysis included the vertebral body, transverse and spinous processes, facet joint, dural sac, ligamentum flavum, psoas muscle, and paraspinal muscle. The final score was determined by taking the average of the scores provided by the two raters.

Statistical Analysis

Continuous variables are expressed as mean ± standard deviation. Statistical analysis was performed using a commercially available software package (SPSS version

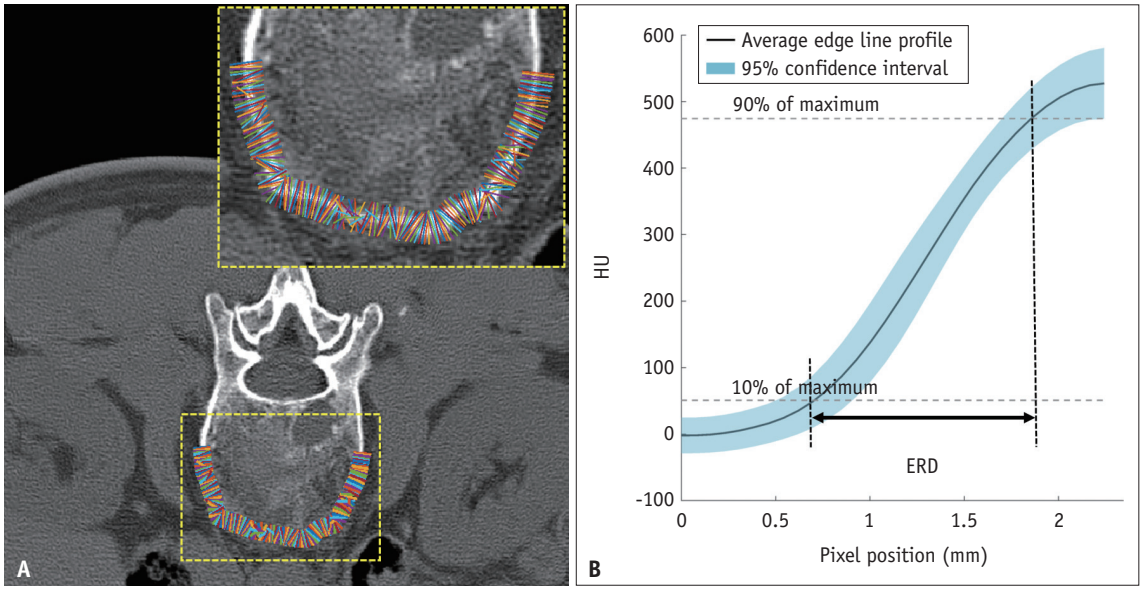

Fig. 1. The process of obtaining ERD.
A. Multiple line segments drawn orthogonal to the vertebral body cortex. **B.** ERD was calculated as the distance between two points at 10% and 90% of maximal intensity on the average edge line profile reflecting the average HU of drawn lines. ERD = edge rise distance, HU = Hounsfield unit

https://doi.org/10.3348/kjr.2021.0140

Korean Journal of Radiology
KJR

25; IBM Corp.). Noise, SNR, ERD, and image quality scores were compared using one-way analysis of variance (ANOVA) followed by a posthoc test using pairwise comparison with Bonferroni correction. The interobserver reliability for subjective indicators was analyzed using a linear weighted kappa coefficient graded as follows: none to slight, < 0.20; fair, 0.21–0.40; moderate, 0.41–0.60; substantial, 0.61–0.80; and excellent, > 0.80 [18]. Statistical significance was set at $p < 0.05$.

RESULTS

Radiation Exposure from CT Scans

The mean volume CT dose index (CTDIvol) and the dose length product (DLP) of the initial survey scans obtained at a radiation dose of 100 mAs were 6.45 ± 0.14 mGy (range, 5.47–6.47) and 103.93 ± 11.5 mGy-cm (range, 97.8–139.9), respectively. The mean CTDIvol and DLP of the intraprocedural scans obtained at a radiation dose of 50 mAs were 3.56 ± 0.1 mGy (range, 3.23–3.59) and 9.3 ± 1.05 mGy-cm (range, 9.0–12.9), respectively.

Quantitative Image Analysis

The results of quantitative image analysis are presented in Table 2. In the paraspinal muscle, the image noise of the denoised 50-mAs images (36.38 ± 7.03 HU) was significantly lower than that of the 50-mAs (93.33 ± 25.36 HU) and 100-mAs (63.33 ± 16.09 HU) images ($p < 0.001$). The SNR was highest for the denoised 50-mAs images (1.46 ± 0.54), followed by the 100-mAs (0.99 ± 0.34) and 50-mAs (0.58 ± 0.18) images ($p < 0.001$).

Edge sharpness was significantly higher in the denoised 50-mAs images than in the 100-mAs images at the margin of the vertebral body (ERD: 0.94 ± 0.2 mm vs. 1.05 ± 0.24 mm, $p = 0.036$) and the psoas muscle (ERD: 0.42 ± 0.09 mm vs. 0.50 ± 0.12 mm, $p = 0.002$). No significant difference in sharpness was observed between the 50-mAs and 100-mAs images (vertebral body, $p = 0.261$; psoas muscle, $p = 0.196$) and between the 50-mAs and the denoised 50-mAs images (vertebral body, $p = 0.632$; psoas muscle, $p = 0.203$) (Table 3).

Qualitative Image Analysis

The subjective overall image quality was significantly higher in the denoised 50-mAs images than in the 50-

Table 1. Subjective Image Quality Assessment Rating

Score	Overall Image Quality	Visibility of Anatomical Structures
1	Markedly noisy, marginally acceptable for the guidance of an access device	Contours are ragged and images are inadequate for diagnostic reporting
2	Quite noisy, but acceptable for the guidance of an access device	Structures can be seen and contours are blurred or serrated
3	Slightly noisy, inferior to standard-dose CT, but providing some diagnostic information	Structures are fairly defined and some contours are blurred
4	Minimal noise, almost equivalent to standard-dose CT	Structures are well defined

Table 2. Image Noise and SNR of the Paraspinal Muscle

Parameter	50 mAs	Denoised 50 mAs	100 mAs	*P* (ANOVA)
Noise, HU	93.33 ± 25.36	36.38 ± 7.03	63.33 ± 16.09	< 0.001*
SNR	0.58 ± 0.18	1.46 ± 0.54	0.99 ± 0.34	< 0.001†

Data are presented as mean ± standard deviation. *Post hoc test revealed that mean noise of denoised 50 mAs images was significantly lower than that of 50 mAs images ($p < 0.001$) and 100 mAs images ($p < 0.001$), †Post hoc test revealed that the mean SNR of denoised 50 mAs images was significantly higher than that of 50 mAs images ($p < 0.001$) and 100 mAs images ($p < 0.001$). ANOVA = analysis of variance, HU = Hounsfield unit, SNR = signal-to-noise ratio

Table 3. Image Sharpness (ERD) of the Vertebral Body and the Psoas Muscle

Structure	50 mAs	Denoised 50 mAs	100 mAs	*P* (ANOVA)
ERD (Vertebral body)	0.98 ± 0.23	0.94 ± 0.20	1.05 ± 0.24	< 0.001*
ERD (Psoas muscle)	0.46 ± 0.13	0.42 ± 0.09	0.50 ± 0.12	0.003†

Data are presented as mean ± standard deviation. Shorter ERD represents a sharper edge. *Post hoc test revealed that the ERD of denoised 50 mAs images was significantly reduced compared with that of 100 mAs images ($p = 0.036$), †Post hoc test revealed that the ERD of denoised 50 mAs images was significantly reduced compared with that of 100 mAs images ($p = 0.002$). ANOVA = analysis of variance, ERD = edge rise distance

https://doi.org/10.3348/kjr.2021.0140

mAs and 100-mAs images ($p < 0.001$). Figure 2 shows the representative 50-mAs, denoised 50-mAs, and 100-mAs images. In addition, the denoised 50-mAs images, compared with the 100-mAs and 50-mAs images ($p < 0.001$), significantly improved the visualization of the normal anatomical structures (vertebral body, transverse and spinous processes, dural sac, ligamentum flavum, psoas muscle, and paraspinal muscle) (Table 4). The interobserver agreement for the subjective image quality scoring was moderate to excellent (weighted kappa = 0.588–0.865) (Table 5). The mean score of each reader is presented in Supplementary Table 1.

DISCUSSION

We applied the DL-based noise reduction technique to

Fig. 2. CT images of a 43-year-old female patient for biopsy of the L5 left superior articular process lesion.
A-C. 50 mAs **(A)**, denoised 50 mAs **(B)**, and 100 mAs **(C)** images of the bone window setting. **D-F.** 50 mAs **(D)**, denoised 50 mAs **(E)**, and 100 mAs **(F)** images of the soft tissue window setting.

Table 4. Subjective Image Quality Analysis

	CT*			Difference of Mean Scores		
	50 mAs (A)	Denoised 50 mAs (B)	100 mAs (C)	|(A)-(B)|	|(A)-(C)|	|(B)-(C)|
Overall image quality	1.95 ± 0.37	3.71 ± 0.32	2.80 ± 0.33	1.76	0.85	0.91
Visibility of anatomical structures						
Vertebral body	2.51 ± 0.55	3.82 ± 0.28	3.21 ± 0.52	1.31	0.70	0.61
Transverse and spinous processes	2.49 ± 0.62	3.70 ± 0.37	3.24 ± 0.46	1.21	0.75	0.46
Facet joint	2.72 ± 0.64	3.54 ± 0.49	3.47 ± 0.54	0.82	0.75	0.07†
Dural sac	1.29 ± 0.35	2.62 ± 0.80	1.90 ± 0.59	1.33	0.61	0.72
Ligamentum flavum	1.43 ± 0.50	2.85 ± 0.68	2.23 ± 0.60	1.42	0.8	0.62
Psoas muscle	1.67 ± 0.44	3.62 ± 0.46	2.64 ± 0.53	1.95	0.97	0.98
Paraspinal muscle	1.70 ± 0.49	3.35 ± 0.53	2.63 ± 0.58	1.65	0.93	0.72

*Data are mean ± standard deviation of the average score of the two reviewers, †Scores were significantly different in all comparisons except for facet joint visualization between (B) and (C).

https://doi.org/10.3348/kjr.2021.0140

Korean Journal of Radiology
KJR

Table 5. Interobserver Reliability for Subjective Image Quality Scores

Imaging Parameters	Weighted Kappa Value		
	50 mAs	Denoised 50 mAs	100 mAs
Overall image quality	0.696	0.590	0.606
Visibility of anatomical structures			
Vertebral body	0.697	0.481	0.713
Transverse and spinous processes	0.772	0.656	0.637
Facet joint	0.865	0.759	0.777
Dural sac	0.588	0.707	0.743
Ligamentum flavum	0.820	0.814	0.785
Psoas muscle	0.747	0.684	0.737
Paraspinal muscle	0.763	0.749	0.814

LD lumbar spine CT images obtained for CT-guided bone biopsy. The results of our study demonstrated a significant improvement of 61% in noise reduction and an increase of 151.7% in SNR through the DL-based reconstruction of 50-mAs lumbar spine CT images. The SNR of the denoised 50-mAs image was even greater than that of the 100-mAs image. For the qualitative evaluation, the proposed technique facilitated an improvement in the overall image quality and the visibility of anatomical structures that included both low- and high-contrast objects. These results were obtained without the expense of decreasing image sharpness.

Several studies have addressed the radiation dose reduction in spine CT. LD lumbar spine CT is helpful in the preoperative and postoperative evaluation of scoliosis [19]. Another study found that LDCT is appropriate for the detection of lytic bone lesions and the assessment of fracture risk in patients with multiple myeloma, representing a significant alternative to conventional skeletal surveys with radiography [20]. Since IR was integrated into the CT protocol, the LDCT of the lumbar spine has been investigated for its potential use in various spinal diseases and it provides acceptable image quality [2-5].

IR can reduce noise, but the problem of texture change, which is described as "artificial," "blotchy," "pixelated," "plastic-like" or "waxy," is often raised [5,6,21]. In other words, there is a trade-off between noise reduction and image sharpness in clinical CT images. Our study used a pre-trained DL model that was fed with simulated low-dose lumbar spine CT images generated from standard-dose lumbar spine CT images and trained to extract only noise components while leaving the other anatomical structures of the lumbar spine unaffected. In this study, the pre-trained model extracted noise component images from real LD lumbar spine CT images, which were subtracted from the input images to produce denoised lumbar spine CT images. Unlike IR, this process is performed only in the image domain; therefore, if noise is extracted and removed, the texture can be prevented from being deformed. As a result, the 50-mAs image with DL-based denoising maintained edge sharpness compared with the original 50-mAs image and was even superior to the 100-mAs image.

Several studies have been conducted on the relationship between radiation dose and sharpness on musculoskeletal CT [4,7,22], but the sharpness was subjectively graded. ERD has been used as a parameter to evaluate sharpness on coronary CT angiography or chest CT [10,23-25]. To the best of our knowledge, this is the first study to measure the sharpness of musculoskeletal CT.

Our DL-based denoising technique, which was based on a modified U-net type CNN model, has already been shown to reduce image noise in coronary CT angiography and ultralow-dose chest CT [10,11]. Given that the DLM we used had been trained for various scanner models and protocols, it can be utilized clinically in any institution. It does not interfere with the workflow because the work progresses so quickly that the computation per patient takes only 5–6 seconds. Therefore, generality and speed are strengths of this technique.

The effective radiation dose for lumbar spine radiography is approximately 1.1 mSv on average [26]. Protocols for standard-dose lumbar CT (300 mAs, 120 kVP, 6–10 mSv) and LD lumbar CT (150 mAs, 120 kVP, 1–4 mSv) have been reported in several studies [1,5,26-29]. Because the initial survey (100 mAs, 120 kVP) and intraprocedural (50 mAs, 120 kVP) scans had different scan lengths in our study, it was not appropriate to directly compare the DLPs or the effective doses. Instead, when the CTDIvols were compared, it was 6.45 ± 0.14 mGy vs. 3.56 ± 0.1 mGy for the standard-dose CT and LDCT, respectively.

Our study has several limitations. First, the hybrid and model-based IRs were not compared. This comparison was not possible because not all raw data were permanently left on the DICOM server. In addition, because the IR implements various image qualities according to the vendor type and strength setting, a much more sophisticated and complex design is required. Second, we analyzed the image quality for the visualization of anatomical structures rather than spinal bone lesions. Unlike the 100-mAs images, the 50-mAs images showed a biospy needle at the level of the

 https://doi.org/10.3348/kjr.2021.0140

spinal bone lesion and did not allow us to compare the image qualities for the spinal lesion. Third, the radiation dose reduction in this study was mathematically assumed and may differ from the actual dose received by the patient. Finally, only the axial scan image was evaluated, as it was obtained for CT-guided biopsy.

In conclusion, this study demonstrated that DL-based reconstruction enabled simultaneous noise reduction and the preservation of edge sharpness on LD lumbar spine CT. Investigations on further radiation dose reduction and the clinical applicability of this technique are warranted.

Supplement

The Supplement is available with this article at https://doi.org/10.3348/kjr.2021.0140.

Conflicts of Interest

One author (Jong Hyo Kim) was a stockholder of ClariPI, but did not have control over any of the data or information submitted for publication. Other authors have no potential conflicts of interest to disclose.

Author Contributions

Conceptualization: Sung Hwan Hong, Jong Hyo Kim. Data curation: Ja-Young Choi, Hee-Dong Chae, Hye Jin Yoo. Formal analysis: Hyunjung Yeoh, Sung Hwan Hong, Chulkyun Ahn. Investigation: Hyunjung Yeoh, Sung Hwan Hong, Chulkyun Ahn, Ja-Young Choi, Hee-Dong Chae, Hye Jin Yoo. Methodology: Jong Hyo Kim, Sung Hwan Hong. Project administration: Sung Hwan Hong. Resources: Chulkyun Ahn. Software: Jong Hyo Kim, Chulkyun Ahn. Supervision: Jong Hyo Kim, Sung Hwan Hong. Validation: Hyunjung Yeoh. Visualization: Hyunjung Yeoh, Chulkyun Ahn. Writing—original draft: Sung Hwan Hong, Hyunjung Yeoh, Chulkyun Ahn. Writing—review & editing: Sung Hwan Hong, Jong Hyo Kim.

ORCID iDs

Hyunjung Yeoh
https://orcid.org/0000-0003-3427-9022
Sung Hwan Hong
https://orcid.org/0000-0003-2302-1341
Chulkyun Ahn
https://orcid.org/0000-0003-2919-4892
Ja-Young Choi
https://orcid.org/0000-0002-3363-0629
Hee-Dong Chae
https://orcid.org/0000-0003-2624-1606
Hye Jin Yoo
https://orcid.org/0000-0002-9704-7870
Jong Hyo Kim
https://orcid.org/0000-0002-5695-4976

REFERENCES

1. Alshamari M, Geijer M, Norrman E, Lidén M, Krauss W, Wilamowski F, et al. Low dose CT of the lumbar spine compared with radiography: a study on image quality with implications for clinical practice. *Acta Radiol* 2016;57:602-611
2. Alshamari M, Geijer M, Norrman E, Lidén M, Krauss W, Jendeberg J, et al. Impact of iterative reconstruction on image quality of low-dose CT of the lumbar spine. *Acta Radiol* 2017;58:702-709
3. Lee SH, Yun SJ, Jo HH, Kim DH, Song JG, Park YS. Diagnostic accuracy of low-dose versus ultra-low-dose CT for lumbar disc disease and facet joint osteoarthritis in patients with low back pain with MRI correlation. *Skeletal Radiol* 2018;47:491-504
4. Lee SH, Yun SJ, Kim DH, Jo HH, Song JG, Park YS. Diagnostic usefulness of low-dose lumbar multi-detector CT with iterative reconstruction in trauma patients: acomparison with standard-dose CT. *Br J Radiol* 2017;90:20170181
5. Yang CH, Wu TH, Lin CJ, Chiou YY, Chen YC, Sheu MH, et al. Knowledge-based iterative model reconstruction technique in computed tomography of lumbar spine lowers radiation dose and improves tissue differentiation for patients with lower back pain. *Eur J Radiol* 2016;85:1757-1764
6. Willemink MJ, Noël PB. The evolution of image reconstruction for CT-from filtered back projection to artificial intelligence. *Eur Radiol* 2019;29:2185-2195
7. Shah A, Rees M, Kar E, Bolton K, Lee V, Panigrahy A. Adaptive statistical iterative reconstruction use for radiation dose reduction in pediatric lower-extremity CT: impact on diagnostic image quality. *Skeletal Radiol* 2018;47:785-793
8. Masamoto K, Fujibayashi S, Otsuki B, Hara K, Fukushima Y, Koizumi K, et al. Utility of thoracolumbar low-dose CT with model-based iterative reconstruction for measuring pedicle diameter using a radiation dose less than a one-time lumbar X-ray. *Spine (Phila Pa 1976)* 2020;45:38-47
9. Mayo-Smith WW, Hara AK, Mahesh M, Sahani DV, Pavlicek W. How I do it: managing radiation dose in CT. *Radiology* 2014;273:657-672
10. Hong JH, Park EA, Lee W, Ahn C, Kim JH. Incremental image noise reduction in coronary CT angiography using a deep learning-based technique with iterative reconstruction. *Korean J Radiol* 2020;21:1165-1177
11. Nam JG, Ahn C, Choi H, Hong W, Park J, Kim JH, et al. Image quality of ultralow-dose chest CT using deep learning

techniques: potential superiority of vendor-agnostic post-processing over vendor-specific techniques. *Eur Radiol* 2021;31:5139-5147
12. U.S. Food and Drug Administration. 510(k) premarket notification. Accessdata.fda.gov Web site. https://www.accessdata.fda.gov/scripts/cdrh/cfdocs/cfPMN/pmn.cfm?ID=K183460. Accessed May 13, 2020
13. Ahn C, Heo C, Kim JH. Combined low-dose simulation and deep learning for CT denoising: application in ultra-low-dose chest CT. Proceedings of SPIE - The International Society for Optical Engineering; 2019 Jan 7-9; Singapore, Singapore: SPIE; 2019; p. 110500E.
14. Kolb M, Storz C, Kim JH, Weiss J, Afat S, Nikolaou K, et al. Effect of a novel denoising technique on image quality and diagnostic accuracy in low-dose CT in patients with suspected appendicitis. *Eur J Radiol* 2019;116:198-204
15. Lim WH, Choi YH, Park JE, Cho YJ, Lee S, Cheon JE, et al. Application of vendor-neutral iterative reconstruction technique to pediatric abdominal computed tomography. *Korean J Radiol* 2019;20:1358-1367
16. Lee S, Choi YH, Cho YJ, Lee SB, Cheon JE, Kim WS, et al. Noise reduction approach in pediatric abdominal CT combining deep learning and dual-energy technique. *Eur Radiol* 2021;31:2218-2226
17. Patro SN, Chakraborty S, Sheikh A. The use of adaptive statistical iterative reconstruction (ASiR) technique in evaluation of patients with cervical spine trauma: impact on radiation dose reduction and image quality. *Br J Radiol* 2016;89:20150082
18. McHugh ML. Interrater reliability: the kappa statistic. *Biochem Med (Zagreb)* 2012;22:276-282
19. Abul-Kasim K, Overgaard A, Maly P, Ohlin A, Gunnarsson M, Sundgren PC. Low-dose helical computed tomography (CT) in the perioperative workup of adolescent idiopathic scoliosis. *Eur Radiol* 2009;19:610-618
20. Horger M, Claussen CD, Bross-Bach U, Vonthein R, Trabold T, Heuschmid M, et al. Whole-body low-dose multidetector row-CT in the diagnosis of multiple myeloma: an alternative to conventional radiography. *Eur J Radiol* 2005;54:289-297
21. Mileto A, Guimaraes LS, McCollough CH, Fletcher JG, Yu L. State of the art in abdominal CT: the limits of iterative reconstruction algorithms. *Radiology* 2019;293:491-503
22. Kim JN, Park HJ, Kim MS, Kook SH, Ham SY, Kim E, et al. Radiation dose reduction in extremity multi-detector CT: a comparison of image quality with a standard dose protocol. *Eur J Radiol* 2021;135:109405
23. Suzuki S, Machida H, Tanaka I, Ueno E. Vascular diameter measurement in CT angiography: comparison of model-based iterative reconstruction and standard filtered back projection algorithms in vitro. *AJR Am J Roentgenol* 2013;200:652-657
24. Tatsugami F, Higaki T, Sakane H, Fukumoto W, Kaichi Y, Iida M, et al. Coronary artery stent evaluation with model-based iterative reconstruction at coronary CT angiography. *Acad Radiol* 2017;24:975-981
25. Tatsugami F, Higaki T, Nakamura Y, Yu Z, Zhou J, Lu Y, et al. Deep learning-based image restoration algorithm for coronary CT angiography. *Eur Radiol* 2019;29:5322-5329
26. Alshamari M, Geijer M, Norrman E, Geijer H. Low-dose computed tomography of the lumbar spine: a phantom study on imaging parameters and image quality. *Acta Radiol* 2014;55:824-832
27. Gervaise A, Osemont B, Lecocq S, Noel A, Micard E, Felblinger J, et al. CT image quality improvement using adaptive iterative dose reduction with wide-volume acquisition on 320-detector CT. *Eur Radiol* 2012;22:295-301
28. Bohy P, de Maertelaer V, Roquigny A, Keyzer C, Tack D, Gevenois PA. Multidetector CT in patients suspected of having lumbar disk herniation: comparison of standard-dose and simulated low-dose techniques. *Radiology* 2007;244:524-531
29. Yang CH, Wu TH, Chiou YY, Hung SC, Lin CJ, Chen YC, et al. Imaging quality and diagnostic reliability of low-dose computed tomography lumbar spine for evaluating patients with spinal disorders. *Spine J* 2014;14:2682-2690

https://doi.org/10.3348/kjr.2021.0140